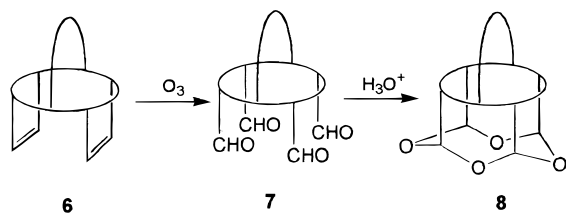
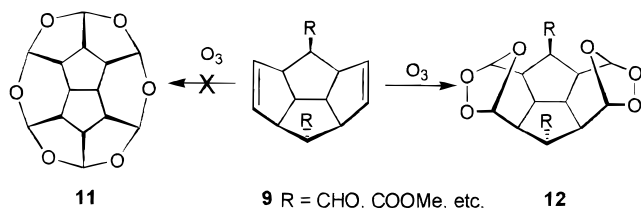




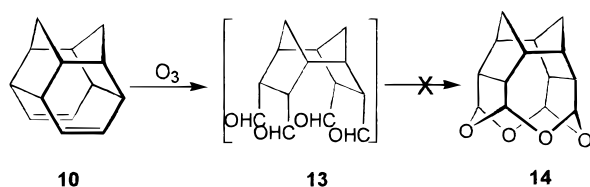
## Scheme 1



## Scheme 2



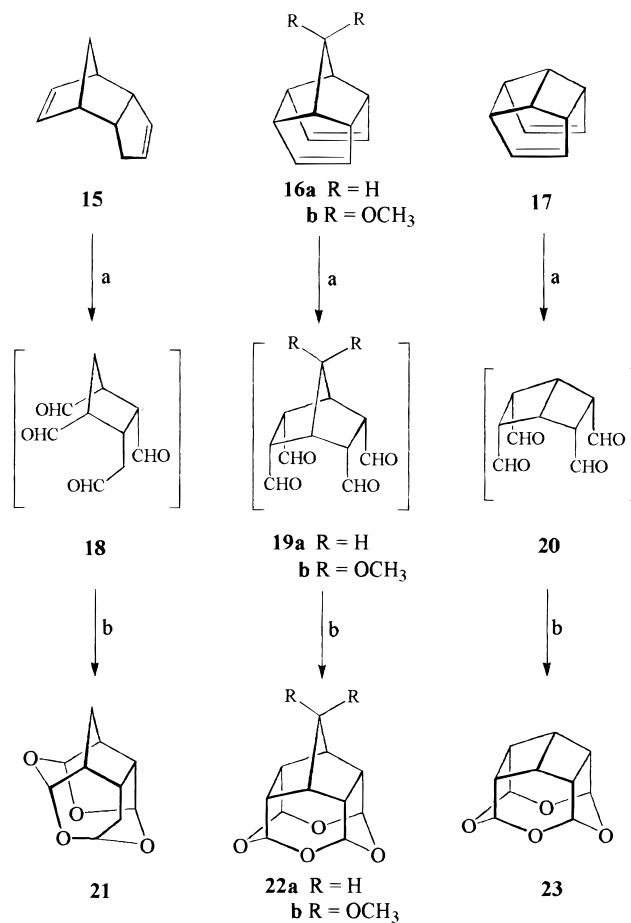
## Scheme 3



To give expression to the theme depicted in Scheme 1, our initial attempts were focused on the tetracyclic diolefin **9**<sup>7</sup> and the pentacyclic diolefin **10**<sup>8</sup> as possible precursors of expanded bowls such as **11** and **14**, respectively. In the event, ozonation of **9** did not lead to the expected *all-cis*-hexaaldehyde and hence to the hexaoxabowl **11** but to an unusually stable diozonide **12** of bowl-like topology, Scheme 2. Formation of several stable diozonides of general structure **12** and elucidation of their structures has been described by us previously.<sup>9</sup> Pentacyclic diolefin **10**<sup>8</sup> was also subjected to ozonolysis with the expectation that the intermediate *all-cis*-tetraaldehyde **13** will undergo in situ cascade cyclization to furnish the corresponding oxa-cage **14** having alternate five- and seven-membered ether rings, Scheme 3. However, we could not isolate any characterizable product except some polymer from this reaction, and this outcome may be due to the unfavorable strain involved in the formation of seven-membered ether rings in **14**.<sup>10</sup> Thus, both size of the rings to be formed and stereochemistry of the aldehyde groups are important in promoting intramolecular acetalization to furnish the corresponding oxa-bowls.

To access relatively smaller oxa-cages having five- and six-membered rings as its walls, following the strategy delineated in Scheme 1, we identified the stereochemically well-defined polycyclic diolefins, dicyclopentadiene **15**, homohypostrophene **16a**,<sup>11</sup> and its functionalized derivative **16b**,<sup>12</sup> and hypostrophene **17**<sup>13</sup> as suitable starting materials. Employing **15**–**17** as the starting

## Scheme 4



a. O<sub>3</sub>, DCM, -78°C; DMS; b. Amberlyst-15, rt, 3–5h

material, we report here the synthesis and characterization of the oxa-cages **21**–**23** and record the interesting observations on the solid-state architecture present in **22a** and **23**.

Our initial efforts were directed toward the commercially available dicyclopentadiene **15**. Ozonolysis of **15** at -78 °C, quenching with dimethyl sulfide, and treatment of the resultant product with Amberlyst-15 furnished **21** as a crystalline solid in 48% yield via cascade intramolecular acetalization in the tetraaldehyde **18**. Structure of **21** was confirmed mainly through incisive analysis of its <sup>1</sup>H and <sup>13</sup>C NMR data, which showed the absence of any symmetry. This preliminary experiment showed that the tetraaldehyde intermediate generated from appropriate precursors does undergo the expected cascade acetalization as depicted in Scheme 1. This encouraged us to prepare homohypostrophene derivatives **16a**<sup>11</sup> and **16b**<sup>12</sup> following literature procedures. Ozonolysis of diolefins **16a** and **16b** and exposure of the intermediates *all-cis*-tetraaldehydes **19a** and **19b** to acid catalyst led to the cyclized tetraoxa compounds **22a** and **22b**, respectively, as the major products in the reaction in ~35% yield, Scheme 4. The structures of oxa-cages **22a,b** were in full consonance with their <sup>1</sup>H and <sup>13</sup>C NMR and MS data. Particularly, the 4 and 5 peaks in the <sup>13</sup>C

(7) (a) Mehta, G.; Srikrishna, A.; Reddy, A. V.; Nair, M. S. *Tetrahedron* **1981**, *37*, 4543. (b) Mehta, G.; Nair, M. S. *J. Am. Chem. Soc.* **1985**, *107*, 7519.

(8) Srikrishna, A.; Sunderbabu, G. *J. Org. Chem.* **1987**, *52*, 5037.

(9) Mehta, G.; Uma, R. *J. Chem. Soc., Chem. Commun.* **1998**, 1735.

(10) Mehta, G.; Vidya, R. Unpublished results.

(11) (a) Underwood, G. R.; Ramamoorthy, B. *J. Chem. Soc., Chem. Commun.* **1970**, 12. (b) Underwood, G. R.; Ramamoorthy, B. *Tetrahedron Lett.* **1970**, 4125.

(12) (a) Eaton, P. E.; Or, Y. S.; Branca, S. J. *J. Am. Chem. Soc.* **1981**, *103*, 2134. (b) Eaton, P. E.; Or, Y. S.; Branca, S. J.; Ravishankar, B. K. *Tetrahedron* **1986**, *42*, 1621.

(13) Paquette, L. A.; Davis, R. F.; James, D. R. *Tetrahedron Lett.* **1974**, 1615.

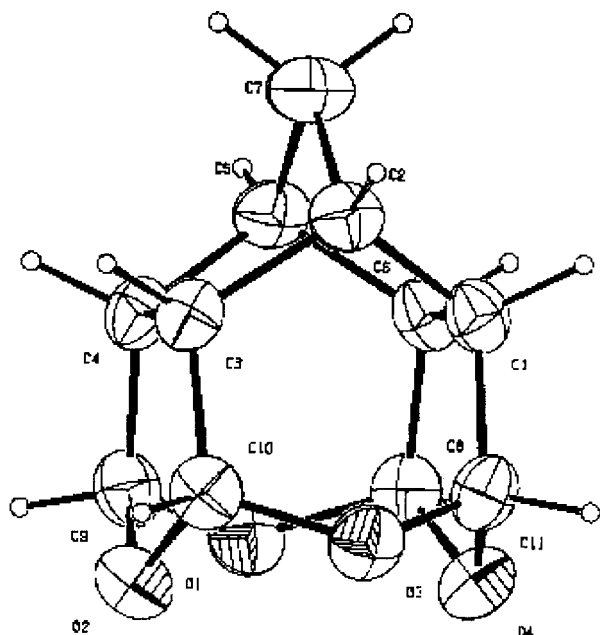


Figure 1. ORTEP diagram of **22a**.

NMR of **22a** and **22b**, respectively, was indicative of the  $C_{2v}$  symmetry present in them. Next, we turned attention toward hypostrophene **17**.<sup>13</sup> Ozonolysis to intermediate *all-cis*-tetraaldehyde **20** and acid catalysis led to 4-fold acetalization and formation of  $C_{2v}$ -symmetric oxa-bowl **23** in 51% yield. The <sup>1</sup>H and <sup>13</sup>C NMR spectra, particularly the presence of three peaks in the latter fully supported the structure **23**.

In our previous studies, the crystal structure of oxa-bowls tetraoxa[4]peristylyane **3** and pentaoxa-[5]-peristylyane **4** showed novel C–H···O-mediated architecture,<sup>3b,4b</sup> and hence, we were interested in studying the solid-state structure of **22a** and **23**. As expected, the single-crystal X-ray analyses of oxa-bowls **22a** and **23** showed some unusual packing patterns sustained through an extensive network of C–H···O interactions.

### Crystal Packing in **22a**

X-ray data (refined by full-matrix least-squares methods on  $F^2$  with the non-H atoms anisotropic and H atoms were placed in calculated positions and were allowed to ride on their parent atoms) revealed that the needle-shaped crystals of **22a** belonged to the chiral space group  $P2_12_12_1$  with four molecules in the unit cell, and the ORTEP diagram of **22a** is shown in Figure 1. The packing pattern reveals a large number of close intermolecular contacts between the molecules. The significant intermolecular C–H···O hydrogen bonds that are within the presently acceptable limits<sup>14</sup> are given in Table 1. The strands of molecules in alternate rim-up, rim-down fashion are arranged perpendicular to the adjacent strands, and this significant arrangement allows the extensive network of C–H···O hydrogen bonds observed in **22a**, Figure 2, viewed along the direction that makes 45° with *a*- and *b*-axes is depicted for reasons of clarity.

When viewed along the *b*-axis, the molecules of **22a** are arranged in alternate rim-up, rim-down fashion in

Table 1. Intermolecular C–H···O Interactions<sup>14</sup> in **22a**

C–H···O	$d(\text{H}\cdots\text{O})$ (Å)	$D(\text{C}\cdots\text{O})$ (Å)	$\theta(\text{C–H}\cdots\text{O})$ (deg)
C1–H1···O3	2.677	3.209	114.4
C1–H1···O4	2.533	3.493	166.3
C2–H2···O1	2.682	3.614	159.0
C4–H4···O1	2.675	3.207	114.4
C4–H4···O2	2.531	3.491	166.3
C5–H5···O3	2.681	3.613	159.0
C9–H9···O4	2.750	3.615	147.4
C11–H11···O2	2.750	3.615	147.5

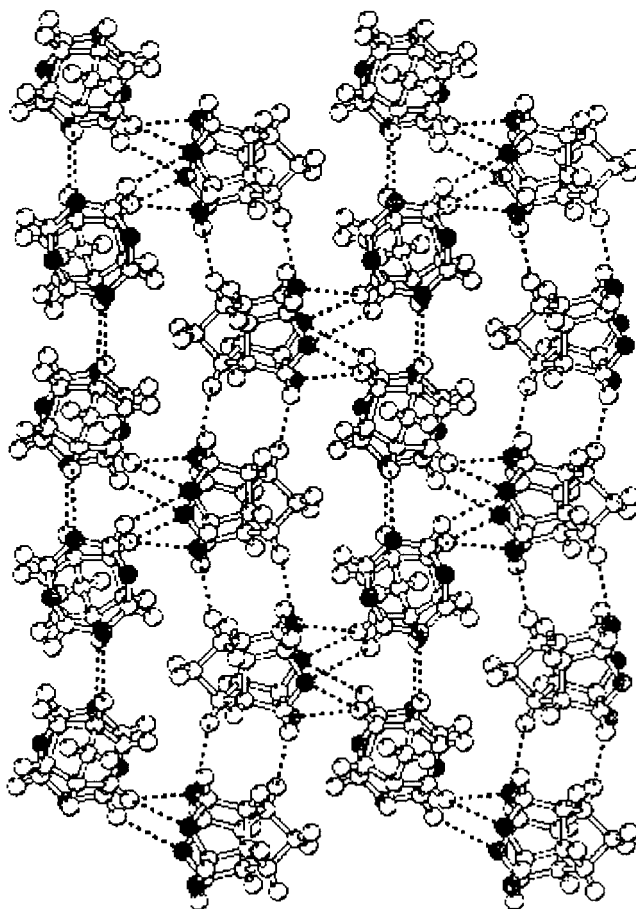


Figure 2. Network of C–H···O interactions in **22a** (view along 45° to the *ab*-plane).

the *ac*-plane. They are interconnected by C–H···O ( $d = 2.68$  Å,  $\theta = 159.0^\circ$ ) hydrogen bonding involving the least acidic bridgehead hydrogen atoms H<sub>2</sub> and H<sub>5</sub> and oxygen atoms O<sub>1</sub> and O<sub>3</sub>, respectively, resulting in a *tape-like motif* of C–H···O hydrogen bonding along the *c*-axis,<sup>15</sup> Figure 3. The C–H···O tapes with molecules arranged in alternate rim-up, rim-down fashion are interconnected through many reasonably strong C–H···O hydrogen bonds, Figure 2.

The least acidic norbornane hydrogen atoms H<sub>1</sub> and H<sub>4</sub> form almost linear hydrogen bonding with acetal oxygen atoms O<sub>4</sub> and O<sub>2</sub> ( $d = 2.53$  Å,  $\theta = 166.3^\circ$ ), respectively, and also with O<sub>3</sub> and O<sub>1</sub> ( $d = 2.68$  Å,  $\theta = 114.4^\circ$ ), respectively. Thus, the hydrogen atoms H<sub>1</sub> and H<sub>4</sub> are involved in bifurcated hydrogen bonding, Figure 2 and Table 1.

The other close contacts observed in the crystal structure of **22a** are C<sub>9</sub>–H<sub>9</sub> with O<sub>4</sub> and C<sub>11</sub>–H<sub>11</sub> with O<sub>2</sub> ( $d =$

(14) (a) Taylor, R.; Kennard, O. *J. Am. Chem. Soc.* **1982**, *104*, 5063. (b) Desiraju, G. R. *J. Chem. Soc., Chem. Commun.* **1990**, 454. (c) Steiner, T. *J. Chem. Soc., Chem. Commun.* **1997**, 727.

(15) Zerkowski, J. A.; MacDonald, J. C.; Seto, C. T.; Wierda, D. A.; Whitesides, G. M. *J. Am. Chem. Soc.* **1994**, *116*, 2382.



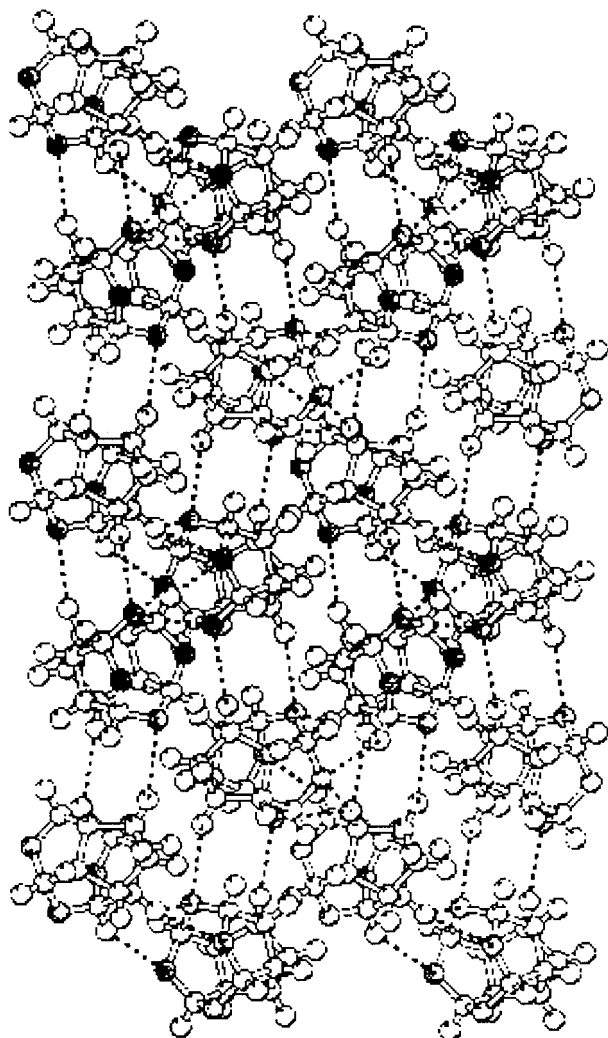


**Figure 3.** Infinite tapelike C–H...O hydrogen-bonding motif along the *c*-axis in **22a**.

2.75 Å,  $\theta = 147.5^\circ$ ) involving the acetal hydrogen atoms. It is noteworthy that only the nonacidic norbornane hydrogen atoms are involved in the formation of reasonably strong C–H...O hydrogen bonds, and the organization of molecules in this crystal corresponds essentially to molecular tapes.

### Crystal Packing in **23**

Slow evaporation of a solution of **23** in THF afforded needle-shaped crystals. Single-crystal X-ray analysis showed that the space group is *Pnma* with only four molecules in the unit cell. It follows that one of the mirror planes of molecule **23** coincides with the crystallographic mirror plane passing through atoms O<sub>1</sub> and O<sub>3</sub> and bisecting the bicyclo[2.2.0]hexane framework. The molecules are tightly packed with high crystal density 1.68 g/cm<sup>3</sup>. Figure 4 portrays the ORTEP perspective of the molecule **23**. The packing pattern reveals a large number of close intermolecular contacts.<sup>14</sup> Only the significant contacts with  $d(\text{H}\cdots\text{O}) < 2.84$  Å are given in Table 2.

When viewed down the *a*-axis, the molecules are arranged in hexagonal close packing with alternate rim-up, rim-down fashion interconnected through C–H...O interaction. The same pattern repeats in next layers but the molecules are slightly displaced with respect to each

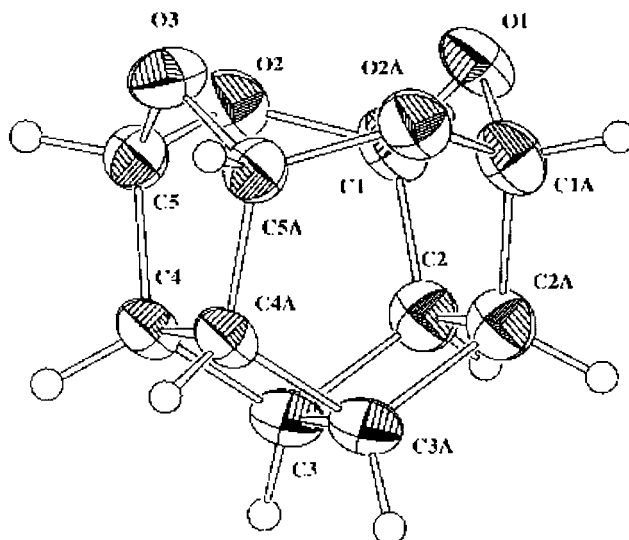


**Figure 4.** ORTEP diagram of **23**.

**Table 2.** Intermolecular C–H...O Interactions<sup>14</sup> in **23**

C–H...O	$d(\text{H}\cdots\text{O})$ (Å)	$D(\text{C}\cdots\text{O})$ (Å)	$\theta(\text{C–H}\cdots\text{O})$ (deg)
C4–H4...O1	2.804	3.533	131.7
C4A–H4A...O1	2.804	3.533	131.7
C4–H4...O2A	2.709	3.590	149.7
C4A–H4A...O2	2.709	3.590	149.7
C3–H3...O3	2.755	3.182	106.9
C3A–H3A...O3	2.755	3.182	106.9
C2–H2...O2	2.837	3.555	130.7
C2A–H2A...O2A	2.837	3.555	130.7

other. This is in contrast to our earlier observation in the molecule pentaoxa[5]peristylane **4**,<sup>4b</sup> where the oxabowls stack exactly on top of each other, in top-to-bottom fashion, forming infinite columnar architecture. This may be due to the fact that the molecule **23** does not possess a flat bottom as pentaoxa[5]peristylane and in this situation the displacement presumably facilitates occurrence of a large number of C–H...O contacts. Though there is no exact bowl-to-bowl stacking in **23**, a large number of bowl-to-bowl C–H...O interactions are present as seen from Figure 5.

When viewed down the *c*-axis, the oxygen atom O<sub>3</sub> makes C–H...O contacts with the less acidic bridgehead hydrogen atoms H<sub>3</sub> and H<sub>3A</sub> ( $d = 2.755$  Å,  $\theta = 106.9^\circ$ ) and O<sub>1</sub> with even lesser acidic cyclobutane hydrogen atoms H<sub>4</sub> and H<sub>4A</sub> ( $d = 2.804$  Å,  $\theta = 131.7^\circ$ ), Figure 5. The oxygen atoms O<sub>2</sub> and O<sub>2A</sub> form C–H...O hydrogen bonds with H<sub>4A</sub> and H<sub>4</sub> ( $d = 2.709$  Å,  $\theta = 149.7^\circ$ ), respectively. These two C–H...O hydrogen bonds, i.e., C<sub>4</sub>–H<sub>4</sub>...O<sub>2A</sub> and C<sub>4A</sub>–H<sub>4A</sub>...O<sub>2</sub>, turn out to be the most significant ones as they hold the oxabowls in top-to-bottom fashion, hence resulting in an *undulated ribbon-like motif* along *a*-axis, Figure 6. The stacks of oxabowls growing in opposite directions along *a*-axis are held together through C<sub>2</sub>–H<sub>2</sub>...O<sub>2</sub> and C<sub>2A</sub>–H<sub>2A</sub>...O<sub>2A</sub> ( $d = 2.837$  Å,  $\theta = 130.7^\circ$ ) close contacts resulting in a *wavelike motif* along *b*-axis, Figure 6.

Thus, all the four oxygen atoms (through both the lone pairs) and all the six least acidic cyclobutane hydrogen atoms of the bicyclo[2.2.0]hexane moiety are involved in a network of C–H...O interactions in molecule **23**. The hydrogen atoms H<sub>4</sub> and H<sub>4A</sub> are involved in bifurcated hydrogen bonding ( $d = 2.709, 2.804$  Å), see Figure 5 and Table 2.

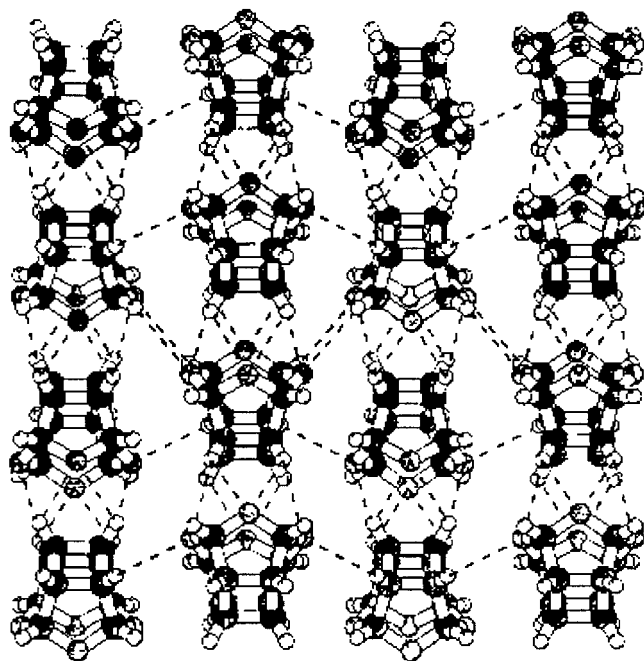


**Figure 5.** Network of C–H···O interactions in the *ab*-plane of **23**.

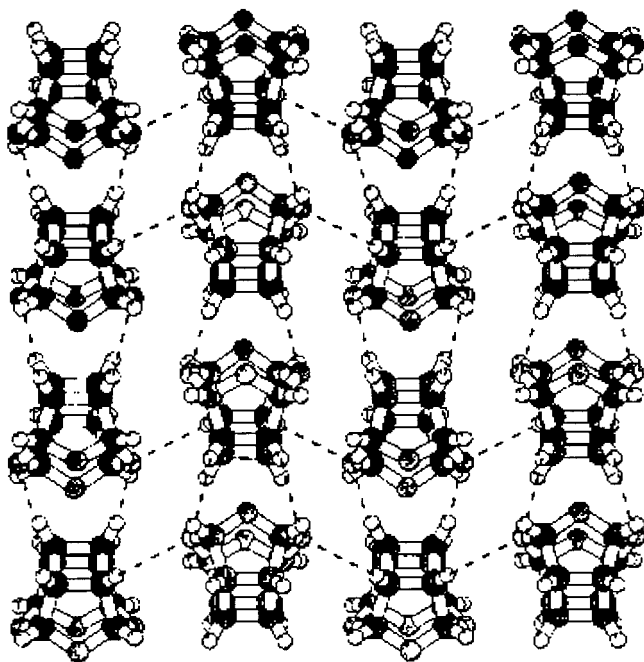


**Figure 6.** "Chain of rings" pattern of C–H···O along the *b*-axis in **23**.

The interesting aspect is the presence of a "chain of rings" pattern<sup>6</sup> of C–H···O hydrogen bonds in the direction of the *b*-axis, Figure 6. This pattern is generated by the combination of two different types of C–H···O motifs involving the oxygen atoms O<sub>2</sub> and O<sub>2A</sub>, namely, an undulated ribbonlike motif along the *a*-axis and a wavelike motif along the *b*-axis. The chains are composed of 10-membered rings linked through the molecules, and each ring is formed around an inversion center. This kind of motif has been observed for the first time in the solid-state structure of oxa-bowls.

It may be of interest to compare the solid-state architecture of the molecules **22a** and **23** with the oxa-peristylanes **3** and **4** described earlier by us.<sup>3b,4b</sup> The common feature observed in the solid-state structure of these molecules is the alternate rim-up, rim-down orientation of molecules and the participation of the least acidic hydrogen atoms in the C–H···O interactions. However, there are significant differences in the C–H···O motifs.

In tetraoxa[4]peristylane **3**, the oxa-bowls are packed in top-to-bottom fashion resulting in columnar arrangement. While there is no direct C–H···O connectivity between the bowls in a column, they are connected laterally to the bowls in adjacent columns resulting in an infinite wavelike C–H···O hydrogen bonding motif. On the other hand, pentaoxa[5]peristylane **4** exhibits bowl-to-bowl columnar arrangement sustained through a C–H···O hydrogen bond resulting in an infinite columnar C–H···O hydrogen bonding motif. In the case of oxa-bowl **23**, there is no exact columnar packing mode due to the slight displacement of the molecules with respect to each other. But, the C–H···O interaction between the bowls in a stack results in an undulated ribbon like C–H···O motif. The topology of the oxa-cage **22a** differs from the oxa-bowls **3**, **4**, and **23** by the presence of a methylene bridge. The organization of molecules in the crystal of **22a** is different and it corresponds essentially to molecular tapes. The molecules are interconnected through a C–H···O hydrogen bond resulting in a tapelike C–H···O motif. Thus, the molecules **3**, **4**, **22a**, and **23** exhibit different C–H···O hydrogen bonding motifs, and this may be attributed to the difference in their molecular symmetry and topology. Interestingly, unlike the oxa-bowls **3** and **4**, in the solid-state structure of both **22a** and **23**, only the nonacidic cycloalkane hydrogen atoms are involved in significant C–H···O interactions and not the relatively more acidic acetal hydrogen atoms.

In summary, we have prepared a new class of oxa-cages **21–23** whose walls are composed of five- and six-membered rings and described the interesting network of C–H···O interactions observed in their solid-state structure.

## Experimental Section

**General Methods.** Melting points are uncorrected. Infrared spectra were recorded as KBr pellets. <sup>1</sup>H NMR spectra were recorded at 300 MHz and <sup>13</sup>C NMR spectra were recorded at 75 MHz, and the NMR samples were made in CDCl<sub>3</sub> solvent. Column chromatography was performed using Acme's silica gel (100–200 mesh), and ethyl acetate–hexane was used as eluent. Commercially available dicyclopentadiene was distilled under vacuum and used for the reaction. Dichloromethane was distilled from calcium hydride.

**Starting Materials.** Diolefins **16a**,<sup>11</sup> **16b**,<sup>12</sup> and **17**<sup>13</sup> were prepared following the literature procedures and duly characterized.

**Tetracyclo[6.3.0.0<sup>2,6</sup>.0<sup>5,9</sup>]undeca-3,10-diene 16a:**<sup>11</sup> <sup>1</sup>H NMR δ 5.90 (s, 4H), 3.16 (s, 2H), 2.40 (s, 4H), 1.68 (s, 2H); <sup>13</sup>C NMR δ 137.1 (CH, 4C), 65.0 (CH, 2C), 49.0 (CH, 4C), 31.7 (CH<sub>2</sub>).

**7,7-Dimethoxytetracyclo[6.3.0.0<sup>2,6</sup>.0<sup>5,9</sup>]undeca-3,10-diene 16b:**<sup>12</sup> <sup>1</sup>H NMR δ 5.92 (s, 4H), 3.36 (s, 6H), 3.20–3.08 (m, 2H), 2.60 (br. s, 4H); <sup>13</sup>C NMR δ 136.5 (CH, 4C), 107.9, 65.0 (CH, 2C), 50.7 (CH<sub>3</sub>, 2C), 46.9 (CH, 4C).

**Tetracyclo[5.3.0.0<sup>2,6</sup>.0<sup>3,10</sup>]deca-4,8-diene 17:**<sup>13</sup> <sup>1</sup>H NMR δ 6.11 (s, 4H), 3.22–3.20 (m, 4H), 3.18–3.12 (m, 2H); <sup>13</sup>C NMR δ 137.5 (CH, 4C), 49.0 (CH, 4C), 43.1 (CH, 2C).

**General Procedure for Ozonolysis.** To a solution of diolefin in dichloromethane (25 mL) at –78 °C was bubbled

(16) Bernstein, J.; Davis, R. E.; Shimoni, L.; Chang, N.-L. *Angew. Chem., Int. Ed. Engl.* **1995**, *34*, 1555.

ozone until the blue color appeared, and the excess ozone was flushed off using oxygen and the ozonide was quenched with dimethyl sulfide (5 equiv) at  $-78\text{ }^{\circ}\text{C}$ . The reaction mixture was stirred with Amberlyst-15 at room temperature for 3–5 h. The resin was filtered off, and the filtrate was concentrated. The residue obtained was passed through a silica gel column to afford the oxa-cages **21**, **22a,b**, **23** in 30–50% yields.

**Spectral Data. 9,11,13,14-Tetraoxapentacyclo[6.5.1.0<sup>2,6</sup>.0<sup>3,12</sup>.0<sup>5,10</sup>]tetradecane 21:** mp 152–153  $^{\circ}\text{C}$ ; IR (KBr) 1209, 1133, 1058  $\text{cm}^{-1}$ ;  $^1\text{H}$  NMR  $\delta$  5.57 (d, 1H,  $J = 6.9$  Hz), 5.48 (d, 1H,  $J = 5.4$  Hz), 5.31 (d, 1H,  $J = 7.2$  Hz), 5.26 (br. s, 1H), 2.97–2.92 (m, 2H), 2.47 (m, 1H), 2.32–2.27 (m, 1H), 1.90–1.88 (m, 3H), 1.51 (td, 1H,  $J_1 = 8.1$  Hz,  $J_2 = 3.9$  Hz);  $^{13}\text{C}$  NMR  $\delta$  103.2, 98.4, 93.6, 88.7, 46.7, 39.3, 39.0, 29.0, 28.4 ( $\text{CH}_2$ ), 25.5 ( $\text{CH}_2$ ); LRMS  $m/z$  197 ( $\text{M}^+ + 1$ ). Anal. Calcd. for  $\text{C}_{10}\text{H}_{12}\text{O}_4$ : C, 61.22; H, 6.17. Found: C, 60.81; H, 6.24.

**9,11,13,14-Tetraoxahexacyclo[6.5.1.1<sup>2,12</sup>.0<sup>3,7</sup>.5<sup>15</sup>.0<sup>6,10</sup>]pentadecane 22a:** mp 230–231  $^{\circ}\text{C}$  dec; IR (KBr) 1098, 1015  $\text{cm}^{-1}$ ;  $^1\text{H}$  NMR  $\delta$  5.44–5.42 (m, 4H), 2.96–2.95 (m, 4H), 2.30–2.29 (m, 2H), 2.21–2.19 (m, 2H);  $^{13}\text{C}$  NMR  $\delta$  95.9 (CH, 4C), 49.6 ( $\text{CH}_2$ , 1C), 43.3 (CH, 4C), 34.9 (CH, 2C); LRMS  $m/z$  209 ( $\text{M}^+ + 1$ ). Anal. Calcd. for  $\text{C}_{11}\text{H}_{12}\text{O}_4$ : C, 63.45; H, 5.81. Found: C, 63.53; H, 5.84.

**4,4-Dimethoxy-9,11,13,14-tetraoxahexacyclo[6.5.1.1<sup>2,12</sup>.0<sup>3,7</sup>.5<sup>15</sup>.0<sup>6,10</sup>]penta decane 22b:** mp 228  $^{\circ}\text{C}$ ; IR (KBr) 1113, 1026  $\text{cm}^{-1}$ ;  $^1\text{H}$  NMR  $\delta$  5.49–5.46 (m, 4H), 3.32 (s, 6H), 3.02–2.99 (m, 4H), 2.34–2.31 (m, 2H);  $^{13}\text{C}$  NMR  $\delta$  121.7 (1C), 96.4 (CH, 4C), 50.8 ( $\text{CH}_3$ , 2C), 39.9 (CH, 4C), 36.7 (CH, 2C); LRMS  $m/z$  268 ( $\text{M}^+$ ). Anal. Calcd for  $\text{C}_{13}\text{H}_{16}\text{O}_6$ : C, 58.20; H, 6.01. Found: C, 58.55; H, 6.13.

**9,11,13,14-Tetraoxahexacyclo[6.5.1.0<sup>2,7</sup>.0<sup>3,6</sup>.0<sup>4,12</sup>.0<sup>5,10</sup>]tetradecane 23:** mp  $> 180\text{ }^{\circ}\text{C}$  dec; IR (KBr) 1115, 1040  $\text{cm}^{-1}$ ;  $^1\text{H}$  NMR  $\delta$  5.55–5.52 (m, 4H), 3.31–3.24 (m, 4H), 2.82–2.73 (m, 2H);  $^{13}\text{C}$  NMR  $\delta$  95.9 (CH, 4C), 34.9 (CH, 4C), 20.7 (CH, 2C); LRMS  $m/z$  195 ( $\text{M}^+ + 1$ ). Anal. Calcd for  $\text{C}_{10}\text{H}_{10}\text{O}_4$ : C, 61.85; H, 5.19. Found: C, 61.84; H, 5.19.

**Crystal data for 22a:**  $\text{C}_{11}\text{H}_{12}\text{O}_4$ ,  $M = 208.21$ , colorless crystals, orthorhombic, space group  $P2_12_12_1$ ,  $a = 8.3520(7)$  Å,  $b = 8.3517(7)$  Å, and  $c = 12.570(8)$  Å,  $V = 876.8(6)$  Å<sup>3</sup>,  $Z = 4$ ,  $D_c = 1.577$  Mg/m<sup>3</sup>,  $T = 293(2)\text{K}$ ,  $F(000) = 440$ ,  $\mu(\text{Mo K}\alpha) = 0.120$  mm<sup>-1</sup>, crystal dimensions  $0.08 \times 0.08 \times 0.18$  mm<sup>3</sup>. Data were collected on an Enraf-Nonius MACH-3 diffractometer, graphite-monochromated Mo K $\alpha$  radiation ( $\lambda = 0.71073$  Å), by  $\omega$  scan method in the range  $2.93 \leq \theta \leq 29.96^{\circ}$ , 2558 unique reflections ( $R_{\text{int}} = 0.0217$ ), of which 1925 had  $F_o > 4\sigma(F_o)$ , were

used in all calculations. At final convergence  $R_1[I > 2\sigma(I)] = 0.0386$ ,  $wR_2 = 0.1006$  for 136 parameters and 0 restraint, GOF = 1.095,  $\Delta\rho_{\text{max}} = 0.187$  e Å<sup>-3</sup>,  $\Delta\rho_{\text{min}} = -0.272$  e Å<sup>-3</sup>. The data were reduced using XTAL (ver 3.4), solved by direct methods, refined by full-matrix least-squares methods on  $F^2$  with the non-H atoms anisotropic, and H atoms were placed in calculated positions and were allowed to ride on their parent atoms.<sup>17</sup>

**Crystal Data for 23:**  $\text{C}_{10}\text{H}_{10}\text{O}_4$ ,  $M = 194.18$ , colorless crystals, orthorhombic, space group  $Pnma$ ,  $a = 10.7635(12)$  Å,  $b = 10.869(7)$  Å, and  $c = 6.5705(16)$  Å,  $V = 768.7(5)$  Å<sup>3</sup>,  $Z = 4$ ,  $D_c = 1.678$  Mg/m<sup>3</sup>,  $T = 293(2)\text{K}$ ,  $F(000) = 408$ ,  $\mu(\text{Mo K}\alpha) = 0.131$  mm<sup>-1</sup>, crystal dimensions  $0.36 \times 0.44 \times 1.28$  mm<sup>3</sup>. Data were collected on an Enraf-Nonius MACH-3 diffractometer, graphite-monochromated Mo K $\alpha$  radiation ( $\lambda = 0.71073$  Å), by  $\omega$  scan method in the range  $3.62 \leq \theta \leq 29.94^{\circ}$ , 1168 unique reflections ( $R_{\text{int}} = 0.00$ ), of which 938 had  $F_o > 4\sigma(F_o)$ , were used in all calculations. At final convergence  $R_1[I > 2\sigma(I)] = 0.0400$ ,  $wR_2 = 0.0950$  for 68 parameters and 0 restraint, GOF = 1.082,  $\Delta\rho_{\text{max}} = 0.303$  e Å<sup>-3</sup>,  $\Delta\rho_{\text{min}} = -0.189$  e Å<sup>-3</sup>. The data were reduced using XTAL (ver 3.4), solved by direct methods, refined by full-matrix least-squares methods on  $F^2$  with the non-H atoms anisotropic, and H atoms were placed in calculated positions and were allowed to ride on their parent atoms.<sup>17</sup>

**Acknowledgment.** We are grateful to Prof. K. Venkatesan for useful discussions. We would like to thank Dr. K. Sekar of Bio-informatics and Interactive Graphics Center of I.I.Sc., Bangalore, for his help in generating the packing diagrams. The crystal data were collected at the National Single Crystal X-ray Facility, University of Hyderabad, Hyderabad. One of us (R.V.) thanks CSIR for a research fellowship.

**Supporting Information Available:** Tables of X-ray crystal data, atomic coordinates, bond lengths, bond angles and anisotropic thermal parameters for **22a** and **23**. This material is available free of charge via the Internet at <http://pubs.acs.org>.

JO0000731

(17) Sheldrick, G. M. SHELX-97, University of Gottingen, Germany.